

Spherical DNA for Probing Wettability of Microplastics

Mohamad Zandieh, Úna E. Hogan, Rodney D.L. Smith and Juewen Liu*

Department of Chemistry, Waterloo Institute for Nanotechnology, University of Waterloo,
Waterloo, Ontario, N2L 3G1, Canada

Email: liujw@uwaterloo.ca

Abstract

Wettability of microplastics may change due to chemical or physical transformations at their surface. In this work, we studied the adsorption of spherical nucleic acids (SNA) with a gold nanoparticle core and linear DNA of the same sequence to probe the wettability of microplastics. Soaking microplastics in water at room temperature for 3 months resulted in the enhancement of SNA adsorption capacity and affinity, whereas linear DNA adsorption was the same on the fresh and soaked microplastics. Drying of the soaked microplastics followed by rehydration decreased the adsorption of SNA, suggesting that the effect of soaking was reversible and related to physical changes instead of chemical changes to the microplastics. Raman spectroscopy data also revealed no chemical transformations of the soaked microplastics. Heating of microplastics over a short period induced a similar effect as long-term soaking. We propose that soaking or heating removes air entrapped in the nanosized pores at the water-plastic interface, increasing the contact surface area of the SNA to afford stronger adsorption. However, such wetted porosity would not change the adsorption of linear DNA because of its much smaller size.

Introduction

Microplastics are submillimeter plastic particles that are either manufactured intentionally for use in cosmetic and cleaning products (primary microplastics) or generated when plastic wastes are shredded via chemical, biological, or mechanical transformations in the environment (secondary microplastics).^{1, 2} Owing to their high surface-to-volume ratio, microplastics adsorb different pollutants in the environment, such as heavy metal ions,^{3, 4} DNA,⁵⁻⁷ and invasive living organisms.^{8, 9} This makes microplastics detrimental to ecosystems¹⁰ and threat to human and animal health.^{11, 12} Understanding the evolution of surface chemistry of microplastic particles in aqueous environments is a critical step for studying the adsorptive behavior and capacity of these pollutants such that risks can be identified and minimized.

Microplastics undergo gradual physical and chemical transformations in environmental water, known as weathering.¹³ Such changes are induced naturally when microplastics are dispersed in environmental waters over a long period of time. In addition, various methods have been utilized to accelerate chemical and physical transformations in microplastics, such as UV and gamma irradiation, oxidation, and high temperature.^{14, 15} The most common changes are the generation of surface polar groups upon oxidation, production of micropores, and changes in the surface roughness, all of which can change the surface properties of microplastics, such as wettability. UV-treated microplastics can increase the adsorption of Cu^{2+} ,¹⁶ and other heavy metal ions,¹⁷ although the adsorption of some hydrophobic organic compounds was decreased.¹⁸ The interaction of treated microplastics with the environment is also changed.^{19, 20}

Wetting, which refers to the ability of a liquid to contact a solid surface, is an important concept in colloid and interface science. Most fresh microplastics have hydrophobic surfaces. When dispersed in water, they may gradually become hydrophilic and thus enhance the wettability by water.⁹ Studies on the wetting of microplastics have been limited due to the irregular morphology of most microparticles. The wettability may change owing to chemical transformations,^{9, 21-23} for which spectroscopic methods can be used to probe changes in the surface chemistry. However, if wettability changes are only due to physical transformations, the quantification of the degree of wettability is more challenging. Upon wetting, the contact angle of the surface may change, which can in turn influence the flotation or sinking behavior of

particles.^{24, 25} Lin et. al. used a camera to record the sinking ratio and velocity of polystyrene microplastics, which required extensive data analysis and was a rather complicated process.²⁴

DNA oligonucleotides have various applications in antisense delivery,²⁶ biosensing,²⁷ catalysis,²⁸ and nanomaterials assembly.²⁹ Spherical nucleic acids (SNA) are interesting structures made of a high density of DNA or RNA oligonucleotides attached to a nanoparticle core, such as a gold nanoparticle (AuNP).³⁰⁻³⁵ The very high extinction coefficient of AuNPs allows visual observation of AuNPs at a low particle concentration. We previously showed that SNA can strongly adsorb onto various materials surfaces, including a few microplastics, due to polyvalent DNA binding interactions.³⁶⁻³⁹

In this study, we investigated changes in the ability of common microplastics to adsorb SNA upon soaking in water. All tested microplastics adsorbed greater amounts of SNA when they were soaked in water for an extended period of time than when the microplastics were freshly prepared. We showed that the enhancement of SNA adsorption reflected improved wettability of microplastics instead of chemical transformations, and that enhanced wettability can be accelerated by heating. This work establishes SNA adsorption as a powerful tool for analyzing the wettability of microplastics.

Materials and Methods

Chemicals. The 21-mer DNA (5'-AAA AAA AAA CCC AGG TTC TCT) with a 3'-carboxyfluorescein (FAM) label, a 5'-thiol (SH) label, or dual 5'-SH and 3'-FAM labels was purchased from Integrated DNA Technologies (IDT, Coralville, IA, USA). Sodium chloride, 4-(2-hydroxyethyl) piperazine-1-ethanesulfonic acid (HEPES), and urea were obtained from Mandel Scientific (Guelph, ON, Canada). Tween 80, potassium cyanide (KCN), H₂O₂ solution (30 wt. %), and hydrochloric acid were obtained from Sigma-Aldrich. Citrate-capped 13 nm AuNPs were synthesized *via* citrate reduction following a reported method.⁴⁰ Milli-Q water was used to prepare all solutions.

Instrumentation. A Raman spectrometer (DeltaNu, Advantage 785) with a 785 nm laser and a 10 s integration time was utilized to acquire Raman spectra and identify the composing materials of the plastic items. Microscopic images of the microplastics were collected using a Nikon Eclipse Ti-S inverted microscope, and transmission electron microscopy (TEM) images were

obtained using a Phillips CM10 100 kV microscope. Scanning electron microscopy (SEM) images of microplastics were taken using a Zeiss Ultra Plus microscope. To avoid charge buildup, the microplastics sample was gold-coated (~10 nm thick) prior to imaging. Fluorescence measurements were performed using a microplate reader (Spark, Tecan) and UV–vis absorption spectroscopy was performed using a spectrometer (Agilent 8453A). Thermogravimetric analysis (TGA) was performed using a TA instrument Q500 with a temperature ramp rate of 2°C/min.

Raman Spectroscopy. Raman spectroscopy of 3-month-soaked, heated and fresh microplastics was carried out using a Renishaw inVia Raman Microscope. A 633 nm laser (Renishaw HeNe laser, 17 mW) was paired with an 1800 lines mm⁻¹ diffraction grating and a 20X microscope objective to record the spectra for each plastic sample between 0 and 4000 cm⁻¹. The data for each sample were acquired as a single spectrum enabled by the Renishaw SynchroScan feature. The laser power was filtered to 50% intensity, and spectra were acquired with 5 accumulations of 10 s each. The raw data files were processed using Renishaw WiRE 5.5 software by subtracting a polynomial baseline, removing any cosmic rays, and normalizing the intensity of the spectra between 0 and 1.

Preparation of Fresh Microplastics. Multiple commonly used plastic items were collected including a plastic container composed of polyethylene (PE), a centrifuge tube composed of polypropylene (PP), plastic spoons composed of polystyrene (PS), a plastic sheet composed of polyvinylchloride (PVC), a plastic dispenser composed of mixed PS/PVC, and a plastic water bottle composed of polyethylene terephthalate (PET). The composing material of the plastics was verified by Raman spectroscopy,^{41, 42} after which they were cut into smaller pieces and washed with ethanol. The plastic pieces were then shredded via mechanical force using a stainless steel grater to acquire microplastics. The microplastics were collected and dried at room temperature overnight using a vacuum dryer. Prior to use in the experiments, the microplastics were dispersed in the water.

Preparation of Wettable Microplastics. Wettable microplastics were obtained by dispersing fresh microplastics in water and storing them in a drawer at room temperature for 3 months. Accelerated wettability of PP microplastics was achieved by heating freshly dispersed PP microplastics in a water bath at various temperatures, typically for 0.5 h.

SNA Preparation. The freezing method was used to prepare SNA.³² Typically, 3 μM of a 5'-SH modified 21-mer DNA was mixed with ~ 10 nM AuNPs (300:1 molar ratio) and the mixture was placed in a freezer (-20 $^{\circ}\text{C}$) for 3 h. The sample was then thawed at room temperature and washed 3 times via centrifugation (14000 rpm, 15 min) at 15 $^{\circ}\text{C}$. To quantify the density of the attached DNA, SNAs were prepared using dual 5'-SH and 3'-FAM labeled DNA. The AuNP core was dissolved by the addition of 10 mM KCN. Finally, the fluorescence intensity of the sample (excitation at 485 nm) was compared to a standard curve, and the DNA concentration and average number of DNA attached to each AuNP were calculated.

DNA and SNA Adsorption. For linear DNA adsorption, 10 nM 3'-FAM DNA was used, whereas for SNA adsorption, 2 nM AuNP (total of ~ 250 nM DNA) was used. These concentrations were chosen to achieve a reliable signal with minimal standard deviations between multiple trials. The DNA samples were incubated with ~ 1 mg/mL of different microplastics in a buffer (200 mM NaCl, 20 mM HEPES, pH 7.6). The incubation times were chosen to be long enough to achieve adsorption equilibrium: 1 h for the linear DNA, 4 h for SNA, and 0.5 h for SNA adsorption on heated samples. The microplastic concentration was optimized to be sufficiently high to ensure that the surface capacity was not a limiting factor for adsorption. The samples were gently agitated during incubation to allow sufficient contact between microplastics and DNA and to prevent the precipitation of the microplastic particles. The samples were then centrifuged (1000 rpm for 2 min). The fluorescence intensity (for linear DNA) and UV-vis absorbance (for SNA) of the supernatants were measured to back calculate the adsorbed DNA/SNA. The fluorescence signal was measured at an excitation of 485 nm and emission of 535 nm for FAM, and the UV-vis absorbance was measured at 520 nm for the 13 nm AuNPs.

SNA Desorption. First, 2 nM SNA (~ 250 nM DNA) was almost completely adsorbed onto ~ 1 mg/mL PET microplastics in a buffer (200 mM NaCl, 20 mM HEPES, pH 7.6) for 4 h. Then, 4 M urea and/or 0.4% Tween 80 was added and incubated with the pre-adsorbed SNA. The samples were gently agitated during incubation to prevent the precipitation of microplastic particles. After 1 h, the samples were centrifuged (1000 rpm, 2 min), and the SNA desorption was quantified based on the enhancement of the absorbance of the supernatant (at 520 nm).

Results and Discussion

Microplastic Preparation and Characterization. Six commonly used plastic objects, such as a plastic spoon and a water bottle, were collected, and Raman spectroscopy identified their composing materials to be PE, PP, PS, PVC, PS/PVC, and PET (Figure S1). Microplastic samples were prepared via mechanical shredding of plastic items. The size and morphology of the microplastics were then observed using an optical microscope (Figure 1A, B and Figure S2). While the samples had a broad shape and size distribution (from 20 μm to 800 μm),⁴³ they all fulfilled the size requirement of microplastics (<1 mm).⁴⁴

The Soaked Microplastics Adsorbed SNA More Efficiently. The microplastics were freshly dispersed in water and compared with those soaked in water at room temperature for 3 months. First, the adsorption of free oligonucleotides (called linear DNA) was studied in the presence of Na^+ , which is the most abundant metal ion in environmental waters.⁴⁵ The adsorption of linear DNA was the same for the fresh and 3-month-soaked microplastics (Figure 1C). No adsorption was observed for PE, PP, PVC, or PS/PVC, whereas ~10% and ~65% of the DNA was adsorbed on PS and PET, respectively. PS and PET have aromatic structures that can stack with DNA bases to promote adsorption.

We then tested the adsorption of SNA consisting of the same DNA sequence with a 5'-thiol label densely immobilized on a 13 nm AuNP core. On average, 125 DNA strands were attached to each AuNP, and the total DNA concentration was ~250 nM in this experiment. Since SNA enhances the overall interactions between DNA and materials via polyvalent binding,^{36, 37} the adsorption of SNA may provide better insights into microplastics that can only weakly adsorb DNA. The absorbance of AuNPs at 520 nm in the supernatant was used to quantify SNA adsorption (Figure 1D, E). Interestingly, SNA adsorption was remarkably enhanced on the soaked microplastics in all cases (Figure 1E, F). In the presence of 200 mM NaCl, SNA adsorption increased on soaked PE (36%), PP (70%), PS (50%), PVC (37%), and PS/PVC (52%) compared to fresh microplastics (Figure 1E, F). The SNA adsorption capacity on PET remained unchanged because the fresh PET microplastics had already adsorbed ~90% of SNA.

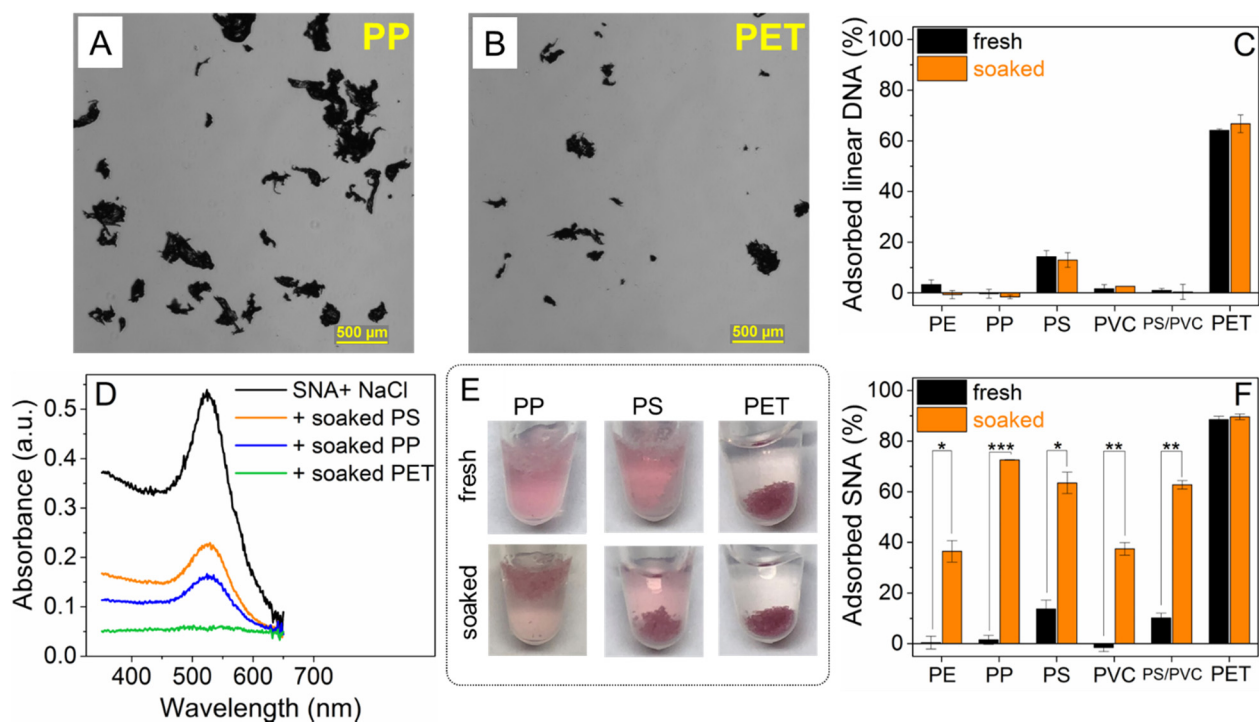


Figure 1. Micrographs of microplastics acquired by shredding plastic materials composed of (A) PP and (B) PET. (C) Adsorption of 10 nM FAM-DNA on freshly prepared and 3-month-soaked microplastics in buffer (200 mM NaCl, 20 mM HEPES, pH 7.6). (D) UV-vis spectra of the supernatants and (E) photographs after adsorption of 2 nM SNA (total of 250 nM DNA) on freshly prepared and 3-month-soaked microplastics. The adsorbed SNA was quantified based on the decrease in the absorbance. (F) Adsorption of 2 nM SNA onto 1 mg/mL of different fresh and soaked microplastics. All experiments shown in this figure were performed in buffer (200 mM NaCl, 20 mM HEPES, pH 7.6). In panel (F), the number of stars represents a significant difference as follows: (*) p -value <0.05 , (**) p -value <0.01 , and (***) p -value <0.001 .

Reversible Change of Wettability. Among the six tested microplastics, PP showed the most dramatic change upon soaking in water (Figure 1F). Therefore, it was investigated for the reason of the enhanced SNA adsorption. We first dried the PP microplastics that were soaked for 3 months and then redispersed them in water immediately before the SNA adsorption experiment. Interestingly, the SNA adsorption efficiency of this dried sample was zero, similar to that of fresh PP microplastics (Figure 2A, green and black curves). This observation suggested that the

enhancement of SNA adsorption was reversible and likely due to physical processes at the microplastic surface instead of irreversible chemical transformations.

Because of their lower density than water, PP microplastics floated on the surface of the water. Figure 2B illustrates the floating behavior of 20 mg of PP microplastics dispersed in 1 mL of water. The dry PP microplastics were hydrophobic based on contact angle measurements ($\sim 108^\circ$, Figure S3). Immediately after dispersing them in water (called fresh PP microplastics), they were located at the top of the water surface, shying away from the water, thereby the majority of them were barely floating. On the other hand, the 3-month-soaked microplastics nicely floated and partially sank close to the surface of the water, suggesting enhanced wettability. Drying and redispersing the microplastics decreased the wettability again, similar to fresh microplastics (Figure 2B). However, it was difficult to visually judge the wettability of microplastics with a density higher than that of water, such as PS/PVC, PVC, and PET (Figure S4).

Raman spectroscopy was used to investigate for any possible changes in functional groups in samples after soaking. Comparing the Raman spectra of the fresh and soaked PP samples, no apparent changes were observed in the carbonyl and hydroxyl regions ($\sim 3000\text{ cm}^{-1}$) confirming that only physical changes occurred, leading to increased wettability (Figure 2C). Oxidation of microplastics can generate surface carbonyl and hydroxyl groups,⁴⁶ which can also enhance adsorption on microplastics.^{6, 17, 47} Previous studies on the oxidation of microplastics typically use remarkably harsher conditions such as heating time of 1-90 days and temperatures of $70\text{-}120^\circ\text{C}$.^{43, 48, 49} For example, when PP microplastics were oxidized at 70°C in the presence of an oxidizing agent ($\text{K}_2\text{S}_2\text{O}_8$), after 5 days, the carbonyl peak started to appear in the IR signal.⁵⁰ Thus, it was not surprising that our mild wetting conditions did not induce a change in the chemistry of the microplastic surface.

We also performed TGA analysis on fresh and 3-month-soaked PP microplastics to investigate their water evaporation behavior. As shown in Figure 2D, water evaporated from the fresh PP samples with a sharper slope, and the temperature at which water fully evaporated was 74°C . In contrast, soaked PP depleted water at 80°C . Therefore, soaked microplastics showed a higher resistance to water evaporation, which could be attributed to the presence of surfaces with stronger affinities to water (e.g., water trapped in pores). After ruling out chemical changes, we

reasoned that a portion of water was able to access pores with smaller features, and those water molecules were more difficult to evaporate because of a higher Laplace pressure. Moreover, when a drop of dye solution was dispensed on top of the fresh microplastics (mixture of PP in water), the droplet remained on the surface (Video S1 and Figure 2E), suggesting that the fresh microplastics contained water away from the surface. In contrast, the soaked microplastics absorbed the dye droplet immediately, suggesting that the water content was close to the microplastic surface.

Therefore, the data in Figure 2 suggested that the enhancement of SNA adsorption on soaked microplastics was reversible and was attributable to the accessibility to small porosities in microplastics. Such wetting of the pores in turn increased the wettability of the microplastics. We reason that when microplastics are freshly dispersed in water, air is trapped at their micro- and nanopores at the surface, making it resistant to wetting and disallowing SNA from coming close to the surface. Over time, these micro- and nanoscale air bubbles break, leading to wetting of the surfaces with nanoscale features to facilitate the adsorption of SNA in the pores.

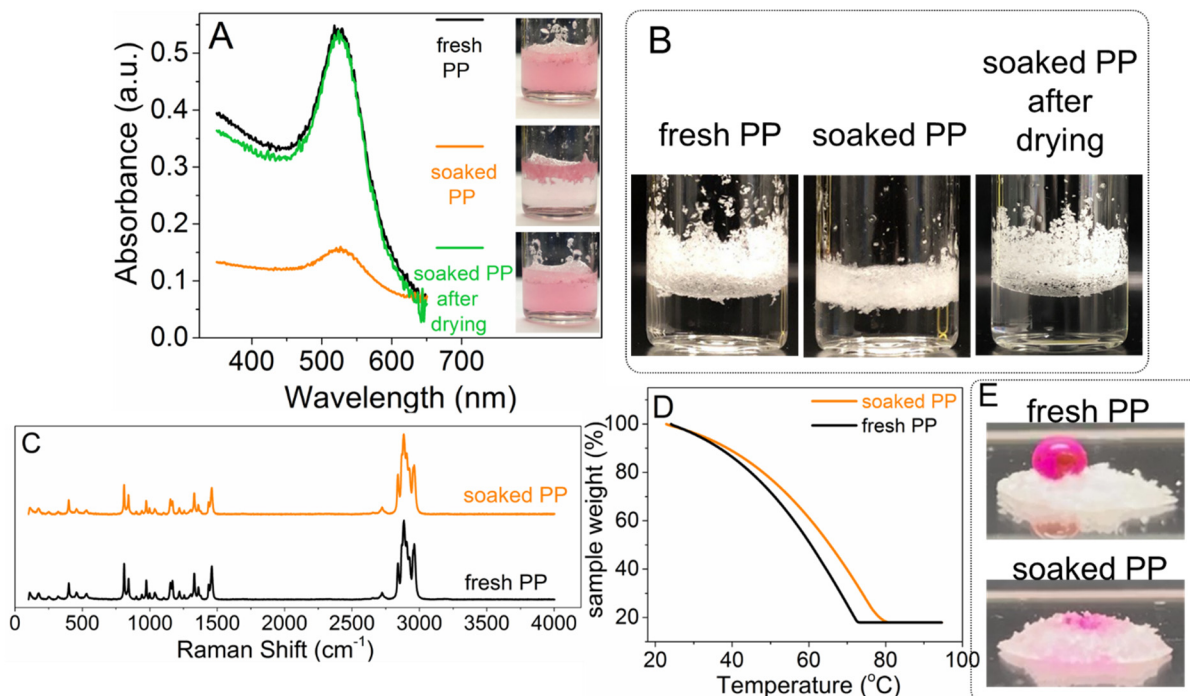


Figure 2. (A) UV–vis spectra of the supernatants and photographs after adsorption of 2 nM SNA (total of 250 nM DNA) on freshly prepared PP, 3-month-soaked PP, and 3-month-soaked PP after drying and redispersion in water. (B) Photographs illustrating the floating behavior of

freshly prepared PP, 3-month-soaked PP, and 3-month-soaked PP after drying and redispersion in water. The soaked PP microplastics showed higher wettability, which accounted for its higher SNA adsorption efficiency. (C) The identical Raman spectra of freshly prepared PP and 3-month-soaked PP suggesting a lack of measurable chemical changes. (D) TGA of ~7 mg of fresh or 3-month-soaked PP microplastics containing ~33 μL of water (a total of 40 mg sample). Upon heating, the water portion evaporated, resulting in weight loss, and dry PP samples were acquired in the end. (E) Photographs illustrating a dye droplet on top of ~7 mg of fresh or 3-month-soaked PP microplastics containing ~13 μL of water (a total of 20 mg sample).

Faster and Stronger Adsorption of SNA by Soaked PET. Because the SNA adsorption capacities of fresh and soaked PET were the same (Figure 1E, F), we further tested the kinetics of SNA adsorption on PET. The kinetic data fitted well with the pseudo-second-order (PSO) adsorption kinetics model, with correlation coefficients (R^2) greater than 0.98 for both fresh and soaked PET (Figure 3A). The SNA adsorption on microplastics was described by the PSO model because the SNA (adsorbate) concentration was relatively low in this experiment and decreased dramatically during the adsorption.⁵¹ As shown in Figure 3A. The adsorption approached a plateau for both microplastics after 2 h and was saturated at ~90% after 4 h. These data are in agreement with the observations shown in Figure 1F. However, based on the kinetic traces, the half-saturation times ($t_{1/2}$) of the fresh and soaked PET were 45 min and 11 min, respectively. Therefore, for PET, the wetting effect was apparent owing to its faster adsorption kinetics.

We further studied the desorption of SNA from fresh and soaked PET to directly compare the adsorption affinities. First, SNA was almost completely adsorbed onto the microplastics after 4 h (Figure S5, red curves). Then, competing agents were added, and desorption was quantified based on the enhancement of the absorbance of the released SNA (Figure S5). Urea (4 M) was used as a hydrogen bonding disrupter to induce desorption. Zero to negligible desorption occurred from both fresh and wet microplastics (Figure 3B). It appeared that strong polyvalent interactions of SNA with both microplastics provided sufficient adsorption stability against urea.

Subsequently, a surfactant (0.4% Tween 80) was added to the pre-adsorbed SNA. Surfactants may use their hydrophobic tail and van der Waals (VDW) forces to adsorb onto microplastics and displace SNA. Interestingly, 76% and 40% of the SNA was desorbed from

fresh and soaked PET, respectively (Figure 3B). These data revealed a range of adsorption affinities for SNA, and more SNA was adsorbed with a higher affinity to the soaked PET than to the fresh PET. Moreover, hydrophobic interactions were likely to be significant for adsorption onto PET. We then added urea and Tween 80 together to reinforce the effect of competing and disrupting agents. SNA was fully desorbed from the fresh PET, whereas only 63% desorption occurred from the soaked PET (Figure 3B), confirming a portion of strongly adsorbed SNA on the soaked PET.

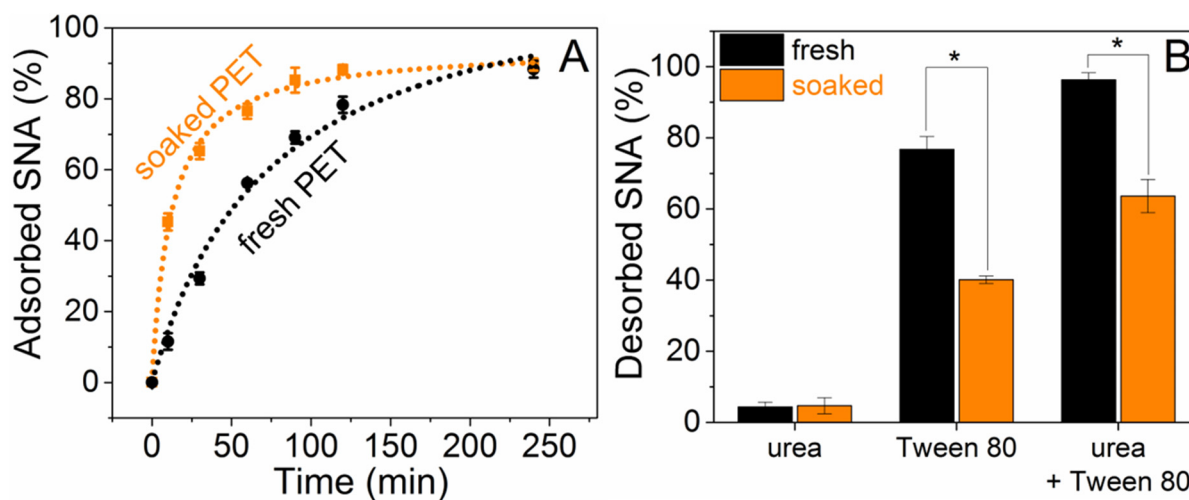


Figure 3. (A) Adsorption kinetics of 2 nM SNA on freshly prepared PET and wettable PET in buffer (200 mM NaCl, 20 mM HEPES, pH 7.6). (B) Desorption of SNA from freshly prepared PET and PET soaked induced by 4 M urea, 0.4% Tween 80, or 4 M urea plus 0.4% Tween 80. In panel B, the number of stars represents a significant difference as follows: (*) p -value<0.05, (**) p -value<0.01, and (***) p -value<0.001.

Accelerated Wetting by Heating. Variation in temperature is a dominant process in the environment,^{14, 52, 53} and we then tested the SNA adsorption on PP microplastics that were heated at various temperatures (50, 60, 70, and 85°C) for 0.5 h. The PP samples heated at 50°C adsorbed slightly more SNA than fresh PP (Figure 4A). When the heating temperature was increased to 60°C and 70°C, the adsorption enhancement was more noticeable, and ~25% of the SNA was adsorbed. Eventually, heating the PP microplastics at 85°C for 0.5 h remarkably increased its SNA adsorption efficiency to 80% (Figure 4A). The floating behavior of PP

microplastics after heating at different temperatures confirmed that their wettability was correlated with the enhanced SNA adsorption (Figure 4B).

The PP microplastics were then heated to different temperatures for a longer duration (3 h). At the same temperature, the adsorption efficiency increased when PP was heated for 3 h instead of 0.5 h (Figure 4A). Overall, heating at higher temperatures or longer times can enhance the SNA adsorption efficiency. Therefore, SNA adsorption can be correlated with different thermal treatment of microplastics, which in turn affected wettability.

Figure 4C shows a TEM image of SNAs adsorbed onto the edge of a PP microplastic particle heated at 85°C. The AuNPs were not evenly distributed but seemed to be concentrated in a few regions, which could be regions with more roughness features and small porosity. A similar distribution of adsorbed SNA was also observed on the 3-month-soaked PP microplastics (Figure S6).

To investigate the origin of the change in these heated samples, we performed Raman spectroscopy on the most harshly heated PP sample (85°C for 3 h). The oxygen-related regions remained unchanged compared to the fresh PP microplastics (Figure 4D). Therefore, similar to the 3-month-soaked PP microplastics, the heated samples did not change chemically. Heating accelerated wetting of the surface compared to that at room temperature.

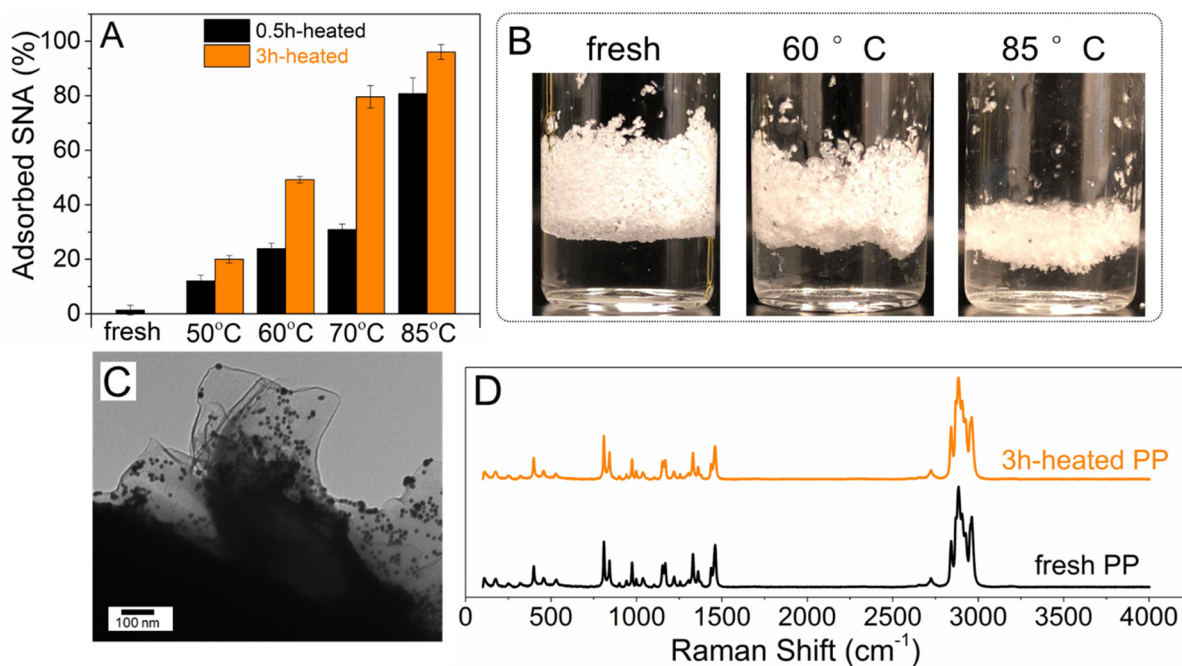


Figure 4. (A) Adsorption 2 nM SNA on the freshly prepared PP and the wettable PP prepared by heating at various temperatures for 0.5 h, or 3 h. The adsorption experiment was performed in buffer (200 mM NaCl, 20 mM HEPES, pH 7.6) for 0.5 h. (B) Photographs illustrating the floating behavior of freshly prepared PP and wettable PP prepared by heating at two different temperatures for 0.5 h. The enhanced wettability of the microplastics accounted for their higher SNA adsorption efficiency. (C) TEM micrograph depicting the SNA adsorbed onto a wettable PP microplastic prepared by heating at 85°C for 0.5 h. (D) Raman spectra of freshly prepared PP and 3 h-heated PP which were identical, suggesting that no chemical change (e.g., oxidation) occurred upon heating the PP microplastics.

Mechanism of SNA adsorption onto Wettable Microplastics. Based on the above results, we believe that microplastics have areas with more roughness features and nanoscale porosity comparable to the size of the SNAs. SEM images of the surface of PP microplastics confirmed the presence of roughness and pores with an average size of a few tens of nanometers (Figure 5A, B), whereas smaller pores might have been covered by the gold coating (~10 nm) step prior to SEM imaging to increase conductivity of the microplastic sample. These surface pores could provide more contact with the SNA, but they easily entrapped air (Figure 5C). Therefore, for fresh microplastics, SNA cannot access the small pores and they contact with the ‘flat’ surface leading to no adsorption (e.g. PP), or loose adsorption (e.g. PET). Soaking allows the wetting of rough surfaces, and SNA can efficiently contact such nanoscale pores (Figure 5D), resulting in a higher adsorption capacity and tighter adsorption via polyvalent binding.

The roughness is still too large for linear DNA, which is why soaking cannot enhance the adsorption of linear DNA (Figure 5E, F). Such an understanding is also potentially applicable to the adsorption of other nanoscale objects and biological agents.

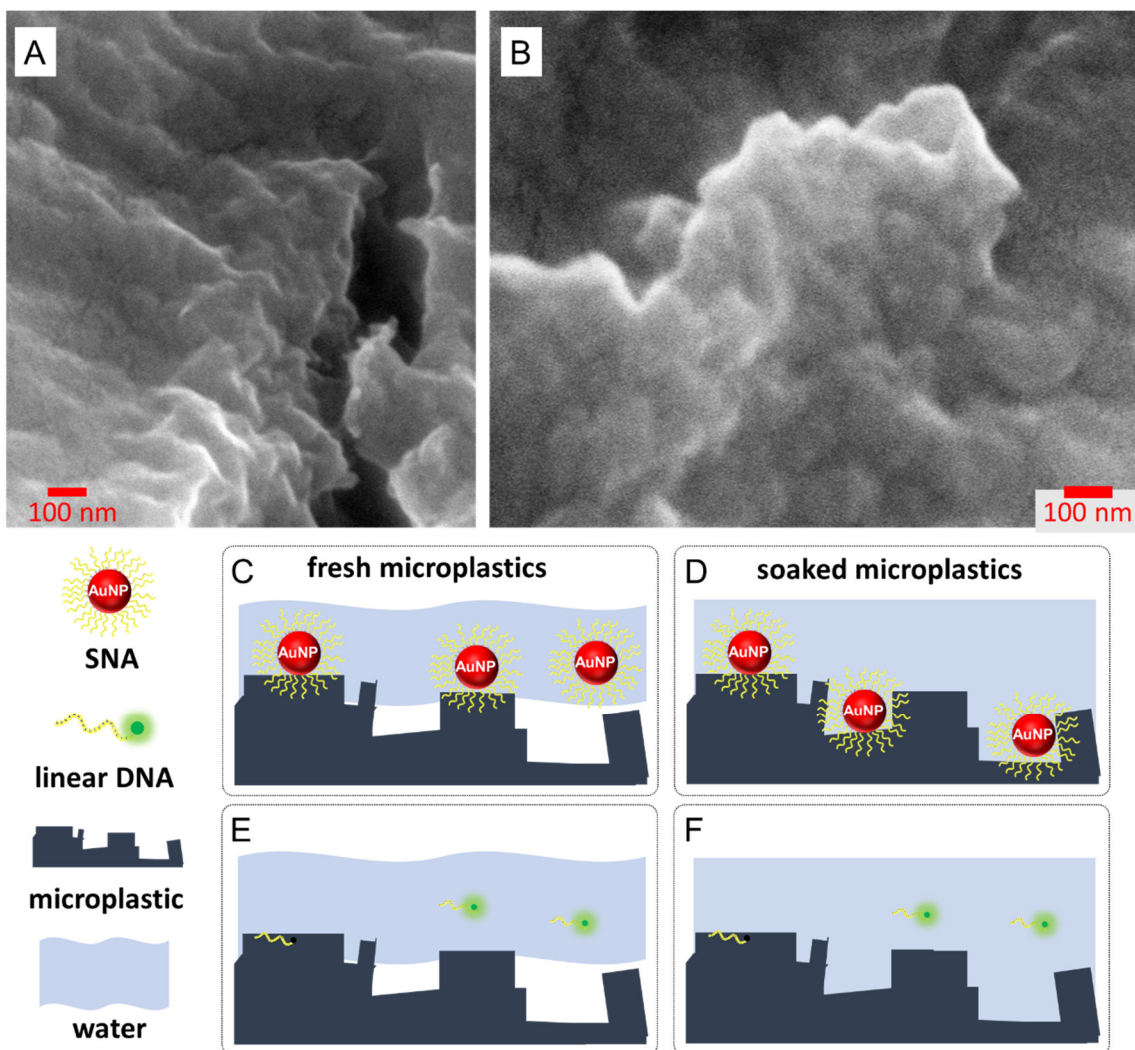


Figure 5. (A, B) SEM micrographs depicting nanoscale roughness and porosity on the surface of the PP microplastics. Schemes illustrating the difference between the (C, D) SNA and (E, F) linear DNA adsorption mechanism on (C, E) fresh microplastics and (D, F) soaked wettable microplastics. Soaking enhances the access of SNA to more surface nanoscale pores, thereby enhancing both the capacity and affinity of adsorption, whereas the roughness features are too large for linear DNA and soaking does not affect its adsorption.

Advantages of the SNA-based Method. While the wettability of PP microplastics can be visually observed as shown in Figure 4B, our SNA-based method has the following advantages and can provide additional information. First, visual observation requires a large quantity of microplastics, which might not be available for environmental samples. With just a few pieces of

microplastics, it is difficult to visually observe the floating behavior, while SNA adsorption can still be measured due to the very high extinction coefficients of AuNps. Second, visual observation works only for light microplastics made of PP (0.90-0.92 g/cm³) or PE (~0.91-0.94 g/cm³), whose density is lower than water. For heavier plastics such as PS (~0.96-1.05 g/cm³) and PVC (~1.1-1.45 g/cm³), they sink in water (Figure S4). Finally, SNA provides a quantitative measurement and we showed a nice correlation between the heating time or temperature and the amount of adsorbed SNA (Figure 4A). Unfortunately, it is difficult to have another way to quantitatively measure wetting of microplastics. We tried to pack a capillary to measure the speed of capillary rise using the Washburn method.⁵⁴ This method is highly dependent on the way of packing the capillary and requires the use of dry samples. However, we need to keep soaked microplastics wet, and we could not obtain a reliable measurement. Thus, the adsorption of SNA provides a unique and convenient way to quantitatively measure wettability of microplastics.

Conclusions

When dispersed in water, microplastics may undergo chemical and/or physical transformations. Although harsh conditions are required to induce chemical transformations, such as oxidation, physical changes may occur under milder conditions. Herein, we observed that the interaction of microplastics with SNA was highly influenced when microplastics were soaked in water at room temperature for 3 months or when they were heated for a few hours. When these microplastics were dried, they behaved similarly to fresh microplastics for SNA adsorption, suggesting a reversible physical change, which was also supported by Raman spectroscopy. Based on the better retention of water by the long-term-soaked microplastics, the effect of soaking was likely related to the access of nanoscale porosity. It was concluded that the surface of the soaked microplastics had more porosity wetted by water, allowing SNA to access these nanoscale features to establish stronger adsorption due to increased contact areas. Based on the observations in this study, adsorption studies need to carefully consider the time- and temperature-dependent changes in microplastics.

Supporting Information

The Supporting Information is available free of charge at <https://pubs.acs.org/doi/10.1021/acs.langmuir.xxxxxxx>.

- Raman spectroscopy characterization of source plastic materials; additional optical micrographs of the microplastic samples; contact angle measurement of PP microplastics; photographs of soaked and fresh PS/PVC microplastics; additional UV-vis spectra for the quantification of released SNA; TEM micrograph of SNA adsorbed on soaked PP (PDF)
- Wetting of fresh and soaked PP (MP4)

Acknowledgements

Funding for this work was provided by the Natural Sciences and Engineering Research Council of Canada (NSERC) Alliance Grants-Plastics Science for a Cleaner Future program (Grant No: ALLRP 558435–20).

References

- (1) Ivleva, N. P., Chemical Analysis of Microplastics and Nanoplastics: Challenges, Advanced Methods, and Perspectives. *Chem. Rev.* **2021**, 121, 11886-11936.
- (2) Jenkins, T.; Persaud, B. D.; Cowger, W.; Szigeti, K.; Roche, D. G.; Clary, E.; Slowinski, S.; Lei, B. J. M.; Abeynayaka, A.; Nyadjro, E. S.; Maes, T.; Hampton, L. T.; Bergmann, M.; Aherne, J.; Mason, S. A.; Honek, J. F.; Rezanezhad, F.; Lusher, A. L.; Booth, A. M.; Smith, R. D. L.; Van Cappellen, P., Current State of Microplastic Pollution Research Data: Trends in Availability and Sources of Open Data. *Front. Environ. Sci.* **2022**, 10, 912107.
- (3) Liu, S.; Huang, J.; Zhang, W.; Shi, L.; Yi, K.; Yu, H.; Zhang, C.; Li, S.; Li, J., Microplastics as a Vehicle of Heavy Metals in Aquatic Environments: A Review of Adsorption Factors, Mechanisms, and Biological Effects. *J. Environ. Manage.* **2022**, 302, 113995.
- (4) Zhao, W. G.; Zhao, P.; Tian, Y. M.; Shen, C. Y.; Li, Z. P.; Peng, P.; Jin, C., Investigation for Synergies of Ionic Strength and Flow Velocity on Colloidal-Sized Microplastic Transport and Deposition in Porous Media Using the Colloidal-Afm Probe. *Langmuir* **2020**, 36, 6292-6303.

- (5) Dong, H.; Chen, Y.; Wang, J.; Zhang, Y.; Zhang, P.; Li, X.; Zou, J.; Zhou, A., Interactions of Microplastics and Antibiotic Resistance Genes and Their Effects on the Aquaculture Environments. *J. Hazard. Mater.* **2021**, 403, 123961.
- (6) Yuan, Q.; Sun, R.; Yu, P.; Cheng, Y.; Wu, W.; Bao, J.; Alvarez, P. J., UV-Aging of Microplastics Increases Proximal Arg Donor-Recipient Adsorption and Leaching of Chemicals That Synergistically Enhance Antibiotic Resistance Propagation. *J. Hazard. Mater.* **2022**, 427, 127895.
- (7) Wu, L.; Patel, K.; Zandieh, M.; Liu, J., Promotion of DNA Adsorption onto Microplastics by Transition Metal Ions. *Microplastics* **2023**, 2, 158-167.
- (8) De Oliveira, T. T. S.; Andreu, I.; Machado, M. C.; Vimbel, G.; Tripathi, A.; Bose, A., Interaction of Cyanobacteria with Nanometer and Micron Sized Polystyrene Particles in Marine and Fresh Water. *Langmuir* **2020**, 36, 3963-3969.
- (9) Al Harraq, A.; Bharti, B., Microplastics through the Lens of Colloid Science. *ACS Environ. Au* **2021**.
- (10) Rech, S.; Borrell, Y.; García-Vazquez, E., Marine Litter as a Vector for Non-Native Species: What We Need to Know. *Marine Pollution Bulletin* **2016**, 113, 40-43.
- (11) Sharma, S.; Chatterjee, S., Microplastic Pollution, a Threat to Marine Ecosystem and Human Health: A Short Review. *Environ. Sci. Pollut. Res.* **2017**, 24, 21530-21547.
- (12) Prata, J. C.; da Costa, J. P.; Lopes, I.; Duarte, A. C.; Rocha-Santos, T., Environmental Exposure to Microplastics: An Overview on Possible Human Health Effects. *Sci. Total Environ.* **2020**, 702, 134455.
- (13) Büks, F.; Kaupenjohann, M., The Impact of Microplastic Weathering on Interactions with the Soil Environment: A Review. *SOIL Discuss.* **2021**, 1-22.
- (14) Liu, P.; Shi, Y.; Wu, X.; Wang, H.; Huang, H.; Guo, X.; Gao, S., Review of the Artificially-Accelerated Aging Technology and Ecological Risk of Microplastics. *Sci. Total Environ.* **2021**, 768, 144969.
- (15) Liu, P.; Qian, L.; Wang, H.; Zhan, X.; Lu, K.; Gu, C.; Gao, S., New Insights into the Aging Behavior of Microplastics Accelerated by Advanced Oxidation Processes. *Environ. Sci. Technol.* **2019**, 53, 3579-3588.

- (16) Han, X.; Vogt, R. D.; Zhou, J.; Zheng, B.; Yu, X.; Feng, J.; Lu, X., Increased Cu (II) Adsorption onto UV-Aged Polyethylene, Polypropylene, and Polyethylene Terephthalate Microplastic Particles in Seawater. *Front. Marine Sci.* **2021**, *8*.
- (17) Mao, R.; Lang, M.; Yu, X.; Wu, R.; Yang, X.; Guo, X., Aging Mechanism of Microplastics with UV Irradiation and Its Effects on the Adsorption of Heavy Metals. *J. Hazard. Mater.* **2020**, *393*, 122515.
- (18) Hüffer, T.; Weniger, A.-K.; Hofmann, T., Sorption of Organic Compounds by Aged Polystyrene Microplastic Particles. *Environ. Pollut.* **2018**, *236*, 218-225.
- (19) Vockenber, T.; Wichard, T.; Ueberschaar, N.; Franke, M.; Stelter, M.; Braeutigam, P., The Sorption Behaviour of Amine Micropollutants on Polyethylene Microplastics—Impact of Aging and Interactions with Green Seaweed. *Environ. Sci. Process. Impacts* **2020**, *22*, 1678-1687.
- (20) Zhang, Y. C.; Su, X. T.; Tam, N. F. Y.; Lao, X. L.; Zhong, M. L.; Wu, Q. H.; Lei, H. F.; Chen, Z. H.; Li, Z.; Fu, J., An Insight into Aggregation Kinetics of Polystyrene Nanoplastics Interaction with Metal Cations. *Chin. Chem. Lett.* **2022**, *33*, 5213-5217.
- (21) Pete, A. J.; Brahana, P. J.; Bello, M.; Benton, M. G.; Bharti, B., Biofilm Formation Influences the Wettability and Settling of Microplastics. *Environ. Sci. Technol. Lett.* **2023**, *10*, 159-164.
- (22) Rius-Ayra, O.; Biserova-Tahchieva, A.; Llorca-Isern, N., Surface-Functionalised Materials for Microplastic Removal. *Mar. Pollut. Bull.* **2021**, *167*, 112335.
- (23) Volgare, M.; De Falco, F.; Avolio, R.; Castaldo, R.; Errico, M. E.; Gentile, G.; Ambrogio, V.; Cocca, M., Washing Load Influences the Microplastic Release from Polyester Fabrics by Affecting Wettability and Mechanical Stress. *Sci. Rep.* **2021**, *11*, 19479.
- (24) Lin, J.; Wu, X.; Liu, Y.; Fu, J.; Chen, Y.; Ou, H., Sinking Behavior of Polystyrene Microplastics after Disinfection. *Chem. Eng. J.* **2022**, *427*, 130908.
- (25) Chen, Y.; Liu, R.; Wu, X.; Liu, Y.; Fu, J.; Ou, H., Surface Characteristic and Sinking Behavior Modifications of Microplastics During Potassium Permanganate Pre-Oxidation. *J. Hazard. Mater.* **2022**, *422*, 126855.
- (26) Shen, X.; Corey, D. R., Chemistry, Mechanism and Clinical Status of Antisense Oligonucleotides and Duplex RNAs. *Nucleic Acids Res.* **2018**, *46*, 1584-1600.

- (27) Dunn, M. R.; Jimenez, R. M.; Chaput, J. C., Analysis of Aptamer Discovery and Technology. *Nat. Rev. Chem.* **2017**, 1, 1-16.
- (28) Lake, R. J.; Yang, Z.; Zhang, J.; Lu, Y., Dnazymes as Activity-Based Sensors for Metal Ions: Recent Applications, Demonstrated Advantages, Current Challenges, and Future Directions. *Acc. Chem. Res.* **2019**, 52, 3275-3286.
- (29) Li, M.; Wang, C.; Di, Z.; Li, H.; Zhang, J.; Xue, W.; Zhao, M.; Zhang, K.; Zhao, Y.; Li, L., Engineering Multifunctional DNA Hybrid Nanospheres through Coordination-Driven Self-Assembly. *Angew. Chem. Int. Ed.* **2019**, 58, 1350-1354.
- (30) Cutler, J. I.; Auyeung, E.; Mirkin, C. A., Spherical Nucleic Acids. *J. Am. Chem. Soc.* **2012**, 134, 1376-1391.
- (31) Liu, B.; Liu, J., Interface-Driven Hybrid Materials Based on DNA-Functionalized Gold Nanoparticles. *Matter* **2019**, 1, 825-847.
- (32) Liu, B.; Liu, J., Freezing Directed Construction of Bio/Nano Interfaces: Reagentless Conjugation, Denser Spherical Nucleic Acids, and Better Nanoflakes. *J. Am. Chem. Soc.* **2017**, 139, 9471-9474.
- (33) Hao, Y.; Li, Y.; Song, L.; Deng, Z., Flash Synthesis of Spherical Nucleic Acids with Record DNA Density. *J. Am. Chem. Soc.* **2021**, 143, 3065–3069.
- (34) Huang, M.; Xiong, E.; Wang, Y.; Hu, M.; Yue, H.; Tian, T.; Zhu, D.; Liu, H.; Zhou, X., Fast Microwave Heating-Based One-Step Synthesis of DNA and RNA Modified Gold Nanoparticles. *Nat. Commun.* **2022**, 13, 1-14.
- (35) Tseng, W.-B.; Hsieh, M.-M.; Chen, C.-H.; Chiu, T.-C.; Tseng, W.-L., Functionalized Gold Nanoparticles for Sensing of Pesticides: A Review. *J. Food Drug Anal.* **2020**, 28, 521–538.
- (36) Liu, B.; Huang, Z.; Liu, J., Polyvalent Spherical Nucleic Acids for Universal Display of Functional DNA with Ultrahigh Stability. *Angew. Chem. Int. Ed.* **2018**, 57, 9439-9442.
- (37) Zandieh, M.; Liu, J., Cooperative Metal Ion-Mediated Adsorption of Spherical Nucleic Acids with a Large Hysteresis. *Langmuir* **2020**, 36, 14324-14332.
- (38) Zandieh, M.; Liu, J., Spherical Nucleic Acid Mediated Functionalization of Polydopamine-Coated Nanoparticles for Selective DNA Extraction and Detection. *Bioconjugate Chem.* **2021**, 32, 801-809.
- (39) Zandieh, M.; Patel, K.; Liu, J., Adsorption of Linear and Spherical DNA Oligonucleotides onto Microplastics. *Langmuir* **2022**, 38, 1915–1922.

- (40) Liu, J.; Lu, Y., Preparation of Aptamer-Linked Gold Nanoparticle Purple Aggregates for Colorimetric Sensing of Analytes. *Nat. Protoc.* **2006**, 1, 246-252.
- (41) Araujo, C. F.; Nolasco, M. M.; Ribeiro, A. M.; Ribeiro-Claro, P. J., Identification of Microplastics Using Raman Spectroscopy: Latest Developments and Future Prospects. *Water Res.* **2018**, 142, 426-440.
- (42) Adarsh, U.; Kartha, V.; Santhosh, C.; Unnikrishnan, V., Spectroscopy: A Promising Tool for Plastic Waste Management. *TrAC Trends Anal. Chem.* **2022**, 116534.
- (43) Zandieh, M.; Liu, J., Removal and Degradation of Microplastics Using the Magnetic and Nanozyme Activities of Bare Iron Oxide Nanoaggregates. *Angew. Chem. Int. Ed.* **2022**, 61, e202212013.
- (44) Ivleva, N. P., Chemical Analysis of Microplastics and Nanoplastics: Challenges, Advanced Methods, and Perspectives. *Chem. Rev.* **2021**, 121, 11886-11936.
- (45) Bretti, C.; Cardiano, P.; Irto, A.; Lando, G.; Milea, D.; Sammartano, S., Interaction of N-Acetyl-L-Cysteine with Na^+ , Ca^{2+} , Mg^{2+} and Zn^{2+} . Thermodynamic Aspects, Chemical Speciation and Sequestering Ability in Natural Fluids. *J. Mol. Liq.* **2020**, 319, 114164.
- (46) Liu, P.; Lu, K.; Li, J.; Wu, X.; Qian, L.; Wang, M.; Gao, S., Effect of Aging on Adsorption Behavior of Polystyrene Microplastics for Pharmaceuticals: Adsorption Mechanism and Role of Aging Intermediates. *J. Hazard. Mater.* **2020**, 384, 121193.
- (47) Wu, X.; Liu, P.; Huang, H.; Gao, S., Adsorption of Triclosan onto Different Aged Polypropylene Microplastics: Critical Effect of Cations. *Sci. Total Environ.* **2020**, 717, 137033.
- (48) Karlsson, T. M.; Hassellöv, M.; Jakubowicz, I., Influence of Thermooxidative Degradation on the in Situ Fate of Polyethylene in Temperate Coastal Waters. *Mar. Pollut. Bull.* **2018**, 135, 187-194.
- (49) Ding, L.; Mao, R.; Ma, S.; Guo, X.; Zhu, L., High Temperature Depended on the Ageing Mechanism of Microplastics under Different Environmental Conditions and Its Effect on the Distribution of Organic Pollutants. *Water Res.* **2020**, 174, 115634.
- (50) Kong, F.; Xu, X.; Xue, Y.; Gao, Y.; Zhang, L.; Wang, L.; Jiang, S.; Zhang, Q., Investigation of the Adsorption of Sulfamethoxazole by Degradable Microplastics Artificially Aged by Chemical Oxidation. *Arch. Environ. Contam. Toxicol.* **2021**, 81, 155-165.
- (51) Azizian, S., Kinetic Models of Sorption: A Theoretical Analysis. *J. Colloid Interface Sci.* **2004**, 276, 47-52.

- (52) Li, Y.; Gao, H.; Qi, Z.; Huang, Z.; Ma, L.; Liu, J., Freezing-Assisted Conjugation of Unmodified Diblock DNA to Hydrogel Nanoparticles and Monoliths for DNA and Hg²⁺ Sensing. *Angew. Chem. Int. Ed.* **2021**, 60, 12985-12991.
- (53) Munno, K.; Helm, P. A.; Jackson, D. A.; Rochman, C.; Sims, A., Impacts of Temperature and Selected Chemical Digestion Methods on Microplastic Particles. *Environ. Toxicol. Chem.* **2018**, 37, 91-98.
- (54) Galet, L.; Patry, S.; Dodds, J., Determination of the wettability of powders by the Washburn capillary rise method with bed preparation by a centrifugal packing technique. *J. Colloid Interface Sci.* **2010**, 346, 470-475.

For Table of Content Graphics

